

Rice husk as inexpensive renewable immobilization carrier for biocatalysts employed in the food, cosmetic and polymer sectors.

Marco Cespugli^a, Simone Lotteria^a, Luciano Navarini^b, Valentina Lonzarich^b, Lorenzo Del Terra^b, Francesca Vita^c, Marina Zweyer^d, Giovanna Baldini^d, Valerio Ferrario^{a§}, Cynthia Ebert^a, Lucia Gardossi^{a*}

^aLaboratory of Applied and Computational Biocatalysis, Dipartimento di Scienze Chimiche e Farmaceutiche, Università degli Studi di Trieste, Via Licio Giorgieri 1, 34127, Trieste, Italy.

^billycaffè S.p.A., via Flavia 110, 34147 Trieste, Italy

^c Department of Life Science, University of Trieste, 34127 Trieste, Italy

^dDepartment of Medical, Surgical, and Health Sciences, University of Trieste, 34149 Trieste, Italy

ELECTRONIC SUPPLEMENTARY INFORMATION

Figure S1. Schematic representation of the chemical method for the oxidation of the cellulosic component of the rice husk employed in the study.

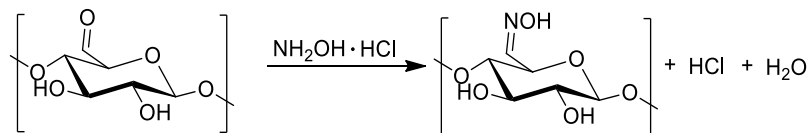


Figure S2: Reaction of cellulose oxidized with hydroxylamine chlorohydrate. The method consists in suspending a certain amount of sample in a concentrated solution of hydroxylamine chlorohydrate for two hours. Available carbonyl groups reacts with a hydroxylamine hydrochloride molecule forming the respective oxime and releasing a hydrochloric acid molecule which is then titrated with sodium hydroxide.

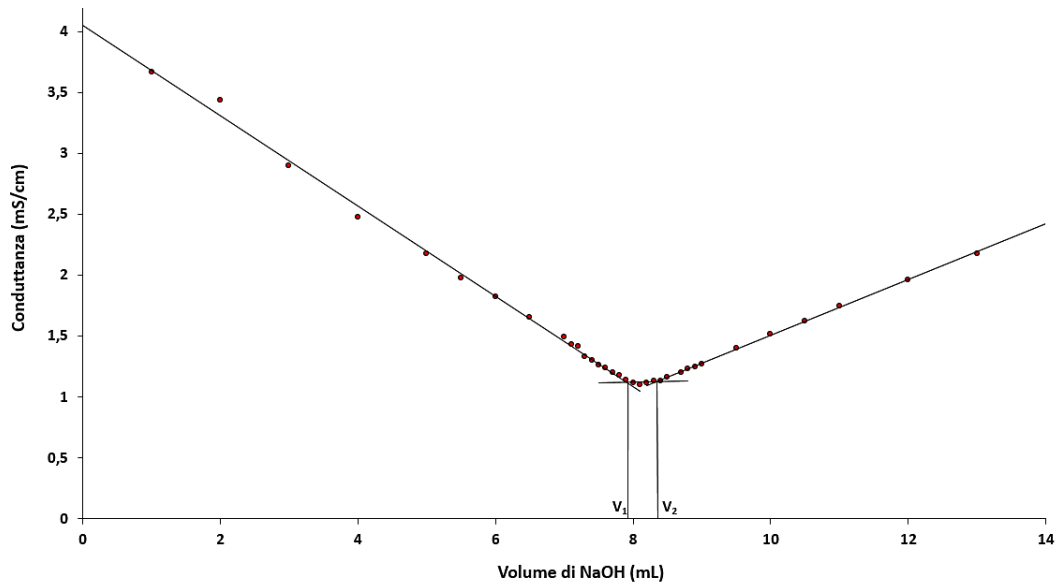


Figure S3: Example of conductimetric titration curve obtained for the titration of oxidized cellulose.

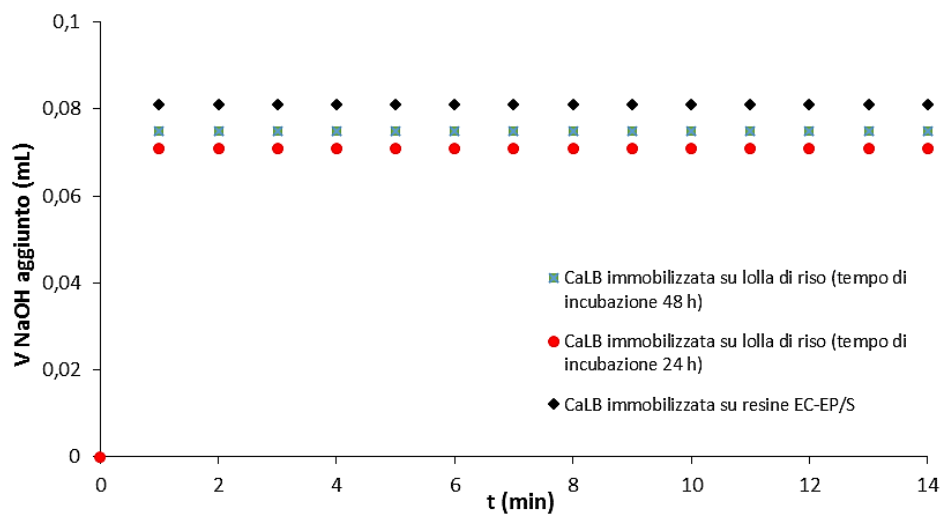


Figure S4: Evaluation of the leaching of the lipase CaLB from the three immobilized preparations upon incubation in the aqueous emulsion used for the lipase hydrolytic assay. Blue: CaLB on EC-EP/S; Red: CaLB on rice-husk with immobilization time= 24h; Light blue: CaLB on EC-EP/S; Red: CaLB on rice-husk with immobilization time= 48h.

Figure S5: Retained activity of CaLB covalently immobilized on RH upon 10 cycles of hydrolytic reactions.

CaLB covalently immobilized on functionalized rice ask applied to the polycondensation of dimethylitaconate and 1,4-butandiol

The following figures report the NMR characterization of the polyesters obtained from the polycondensation of dimethylitaconate (DMI) and 1,4-butandiol (BDO) catalyzed by CaLB immobilized on RH (Figures S6,S7,S8). Percentage conversion was related to the increase in the intensity of the signal (time 24, 48 and 72h) of the methylene H_e protons adjacent to the ester function with the sum of the intensity of the H_e and H_c signals.

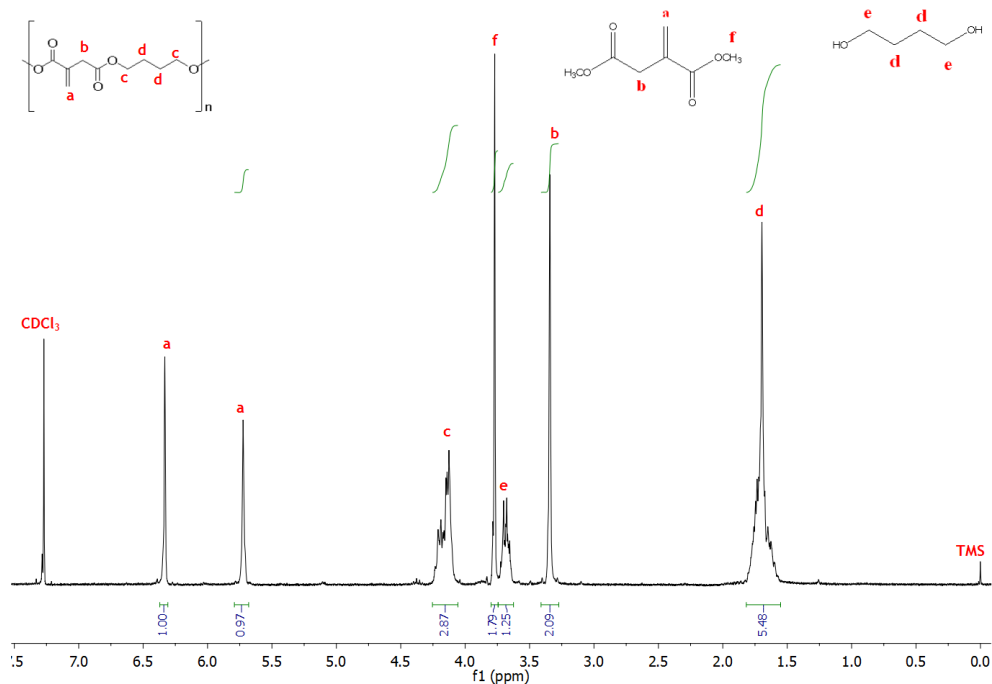


Figure S6: ¹H-NMR spectrum (CDCl₃, 270 MHz) of the polycondensation reaction between dimethyl itaconate (DMI) and 1,4-butanediol (BDO) catalyzed by CaLB immobilized on rice husk after 24h. ¹H-NMR (270MHz, CDCl₃), δ : 1.69 (5.48 H, m, -CH₂CH₂OH), 3.34 (2.09 H, s, -CH₂CO), 3.68 (1.25 H, m, -CH₂CH₂OH), 3.76 (1.79 H, s, -C=CH₂-CO-OCH₃), 4.16 (2.87 H, m, -CH₂OCO-), 5.73 (0.97H, s, -COC=CHH-), 6.33 (1H, s, -COC=CHH-).

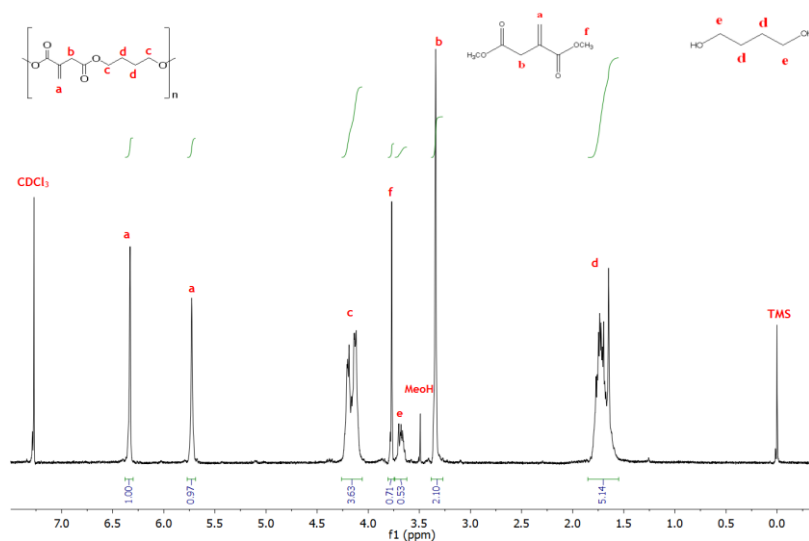


Figure S7: ¹H-NMR spectrum (CDCl₃, 270 MHz) of the polycondensation reaction between dimethyl itaconate and CaLB catalyzed 1,4-butanediol immobilized on rice husk after 48 h. δ : 1.69 (5.14 H, m, -CH₂CH₂OH), 3.34 (2.10 H, s, -CH₂CO), 3.68 (0.53 H, m, -CH₂CH₂OH), 3.76 (0.71 H, s, -C=CH₂-CO-OCH₃), 4.16 (3.63 H, m, -CH₂OCO-), 5.73 (0.97H, s, -COC=CHH-), 6.33 (1H, s, -COC=CHH-).

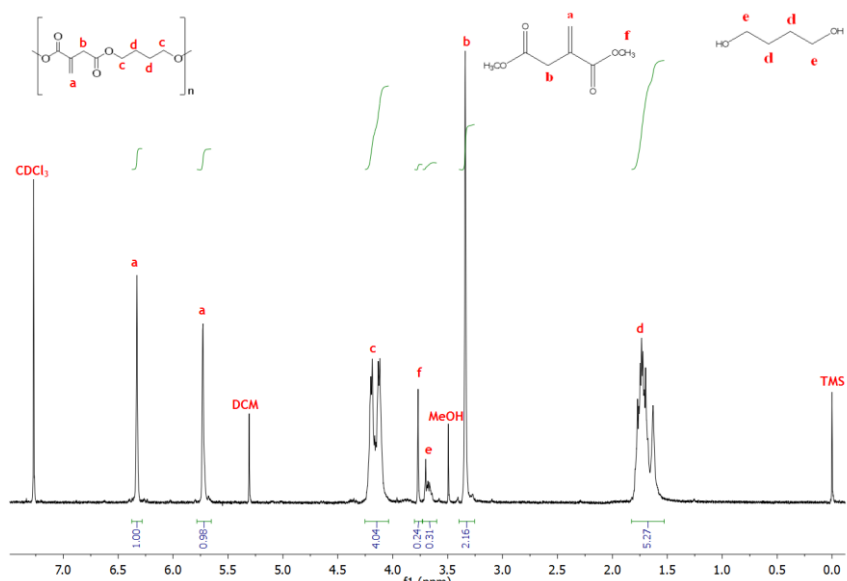


Figure S8: $^1\text{H-NMR}$ spectrum (CDCl_3 , 270 MHz) of the polycondensation reaction between dimethyl itaconate and CaLB catalyzed 1,4-butanediol immobilized on rice husk after 72 h.

δ (ppm): 1,69 (5,27 H, m, $-\text{CH}_2\text{CH}_2\text{OH}$), 3,34 (2,16 H, s, $-\text{CH}_2\text{CO}$), 3,68 (0,31 H, m, $-\text{CH}_2\text{CH}_2\text{OH}$), 3,76 (0,24 H, s, $-\text{CH}_2\text{CO-OCH}_3$), 4,16 (4,04 H, m, $-\text{CH}_2\text{OCO-}$), 5,73 (0,98 H, s, $-\text{COC}=\text{CHH-}$), 6,33 (1H, s, $-\text{COC}=\text{CHH-}$).

CaLB covalently immobilized on EC-EP resin applied to the polycondensation of dimethylitaconate and 1,4-butanediol.

The following figures (Figures S9, S10, S11) report the NMR characterization of the polyesters obtained from the polycondensation of dimethylitaconate (DMI) and 1,4-butanediol (BDO) catalyzed by CaLB immobilized on EC-EP resins. Percentage of conversion was related to the increase in the intensity of the signal (time 24, 48 and 72h) of the methylene H_e protons adjacent to the ester function with the sum of the intensity of the H_e and H_c signals.

Figure S9: $^1\text{H-NMR}$ spectrum (CDCl_3 , 270 MHz) of the polycondensation reaction between dimethyl itaconate and CaLB catalyzed 1,4-butanediol immobilized on EC-EP/S resins after 24 h.

$^1\text{H-NMR}$ (270MHz, CDCl_3), δ : 1.69 (6.79 H, m, $-\text{CH}_2\text{CH}_2\text{OH}$), 3.34 (2.38 H, s, $-\text{CH}_2\text{CO}$), 3.68 (1.39 H, m, $-\text{CH}_2\text{CH}_2\text{OH}$), 3.76 (1.98 H, s, $-\text{C}=\text{CH}_2\text{-CO-OCH}_3$), 4.14 (3.39 H, m, $-\text{CH}_2\text{OCO-}$), 5.73 (1.00 H, s, $-\text{COC}=\text{CHH-}$), 6.33 (1.09 H, s, $-\text{COC}=\text{CHH-}$).

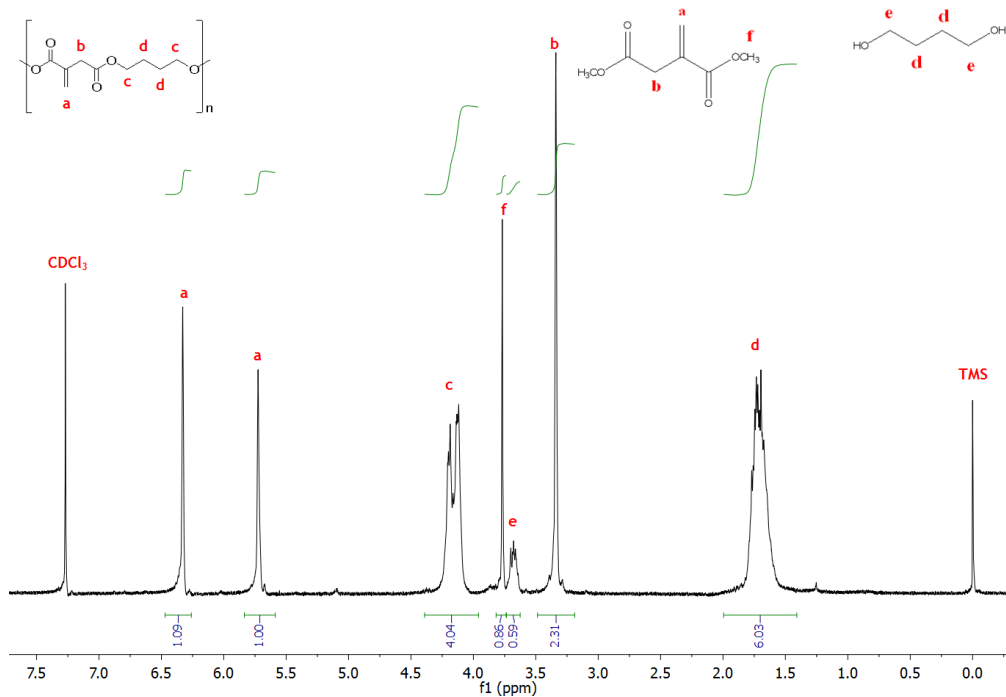


Figure 10: $^1\text{H-NMR}$ spectrum (CDCl_3 , 270 MHz) of the polycondensation reaction between dimethyl itaconate and CaLB catalyzed 1,4-butanediol immobilized on EC-EP/S resins after 48 h.

$^1\text{H-NMR}$ (270MHz, CDCl_3), δ : 1.69 (6.03 H, m, $-\text{CH}_2\text{CH}_2\text{OH}$), 3.34 (2.31 H, s, $-\text{CH}_2\text{CO}$), 3.68 (0.59 H, m, $-\text{CH}_2\text{CH}_2\text{OH}$), 3.76 (0.86 H, s, $-\text{C}=\text{CH}_2\text{-CO-OCH}_3$), 4.14 (4.04 H, m, $-\text{CH}_2\text{OCO-}$), 5.73 (1.00 H, s, $-\text{COC}=\text{CHH-}$), 6.33 (1.09 H, s, $-\text{COC}=\text{CHH-}$).

Figure S11: $^1\text{H-NMR}$ spectrum (CDCl_3 , 270 MHz) of the polycondensation reaction between dimethyl itaconate and CaLB catalyzed 1,4-butanediol immobilized on EC-EP/S resins after 72 h.

$^1\text{H-NMR}$ (270MHz, CDCl_3), δ : 1.69 (5.27 H, m, $-\text{CH}_2\text{CH}_2\text{OH}$), 3.34 (2.16 H, s, $-\text{CH}_2\text{CO}$), 3.68 (0.31 H, m, $-\text{CH}_2\text{CH}_2\text{OH}$), 3.76 (0.24 H, s, $-\text{C}=\text{CH}_2\text{-CO-OCH}_3$), 4.16 (4.04 H, m, $-\text{CH}_2\text{OCO-}$), 5.73 (0.98 H, s, $-\text{COC}=\text{CHH-}$), 6.33 (1H, s, $-\text{COC}=\text{CHH-}$).

```

Name: 1JSL_A_PDBID_CHAIN_SEQUENCE      Length: 327
ADKLPNIVILATGGTIAGSAATGTQTGYKAGALGVDTLINAVPEVKKLANVKGEQFSNMASENMTGDVVVLKLSQRVNEL      80
LARDDVDGVVITHGTDTVESAYFLHLTVKSDKPFVVFVAAMRPATAISADGPMNLLEAVRVAGDKQSRGRGVMVVINDRI      160
GSARYITKTNASTLDTFRANEEGYLGVIIGNRIYYQNRIDKLHTTRSVFDVRGLTSLPKVDILYGYQDDPEYLYDAAIQH      240
GVKGIVYAGMGAGSVSVRGIAGMRKALEKGVVVMRSTRTNGNIVPPDEELPGLVSDSLNPAHARILLMLALTRTSDPKVI      320
QEYFHTY
.....N.....      80
.....      160
.....      240
.....      320
.....      400

(Threshold=0.5)
-----
SeqName      Position  Potential  Jury   N-Glyc
              agreement result
-----
1JSL_A_PDBID_CHAIN_SEQUENCE  64 NMTG  0.6240  (8/9)  +
1JSL_A_PDBID_CHAIN_SEQUENCE  170 NAST  0.3138  (8/9)  --
-----

```

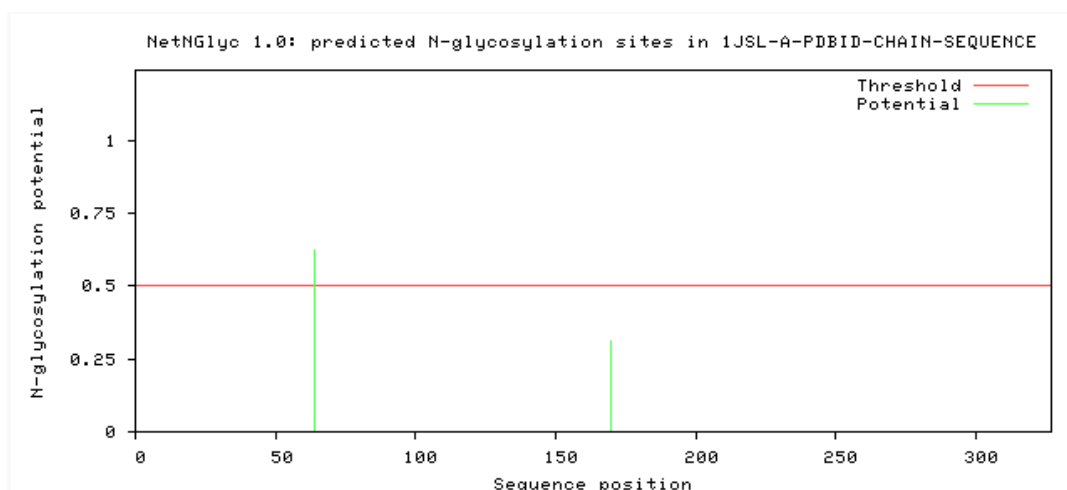


Figure S12: Analysis of the primary structure of asparaginase from *Eriwinia chrysantemi* using the open source software NetNGlyc (<http://www.cbs.dtu.dk/services/NetNGlyc/>) that identifies N-glycosylation sites